Preprints of the 19th World Congress
The International Federation of Automatic Control
Cape Town, South Africa. August 24-29, 2014

Three-Dimensional Nonlinear Path-Following Guidance Law Based on Differential Geometry

Namhoon Cho * **Youdan Kim** ** **Sanghyuk Park** ***

* *Department of Mechanical and Aerospace Engineering, Seoul National University, Seoul, Korea (e-mail: nhcho91@snu.ac.kr)*
** *Department of Mechanical and Aerospace Engineering, Seoul National University, Seoul, Korea (e-mail: ydkim@snu.ac.kr)*
*** *Department of Aerospace and Mechanical Engineering, Korea Aerospace University, Goyang-city, Korea (e-mail: park@kau.ac.kr)*

Abstract: A new three-dimensional nonlinear path-following guidance law is proposed using differential geometry. The guidance law is designed based on the look-ahead angle and the radially shifted distance which gives an additional degree of freedom to generate acceleration command for precise path-following. A modified Frenet-Serret frame is utilized to describe the desired path, and the closest projection point is taken as a reference point on the desired path. To implement the guidance law for the vehicle in a flow-field, a command modifying logic is proposed to generate the sideways command which is orthogonal to the flow-relative velocity. Numerical simulations are performed to verify the performance of the proposed guidance law.

Keywords: Path-Following, Guidance Law, Look-Ahead Angle, Frenet-Serret Frame.

1. INTRODUCTION

The path-following problem can be stated as follows; "*Design a guidance command that makes the vehicle to track the desired path.*" The path-following is one of the important problems for the autonomous operation of the unmanned vehicles. Recently, the missions involving the autonomous flight of the UAV(Unmanned Aerial Vehicle) have become more complicated, and therefore a precise and effective three-dimensional path-following guidance law is especially required.

Various guidance laws have been developed for the purpose of the path-following. Most of the methods have been developed for two-dimensional path-following, which can be classified into three approaches; the error kinematics/dynamics based approach, the vector field based approach, and the virtual target following approach.

In the error kinematics/dynamics based approach, various control laws have been applied where error variables are defined considering the problem of the path-following. The kinematic/dynamic model of the error variables are derived, and linear or nonlinear control design methods are applied to regulate the errors. (Cabecinhas et al. (2007); Gates (2010)) The merits of this approach are the guaranteed stability and the reliable tracking performance from the direct error feedback. However, the guidance command is somewhat complicated and model dependent. Also, a singularity problem may restrict the set of feasible initial conditions.

In the vector field based approach, a vector field designating the desired course angle or velocity at each point is constructed so that the vehicle converges to the desired path along the vector field. (Nelson et al. (2007); Lawrence et al. (2008)) The strength of this approach is the global convergence for the following of straight line and circle paths. However, this approach is not applicable to general space curves.

In the virtual target following approach, or 'Look-ahead point based approach', guidance command is designed to track a virtual target point on the desired path. (Park et al. (2007); Curry et al. (2013); Yamasaki et al. (2013)) This approach was originated from the classical line-of-sight guidance laws. The strengths of this approach are the simplicity of the guidance command, the model independence, and the so-called 'look-ahead effect' which enables tight tracking and wind effect compensation. Taking the look-ahead point as the reference point also provides robustness against the external disturbances. However, the initial position of the vehicle should be inside of the specified look-ahead distance from the desired path, and the look-ahead point is not easy to determine when the desired path is a combination of different types of complicated curves.

In this study, to deal with the weaknesses of the existing path-following guidance laws, a three-dimensional nonlinear path-following guidance law is proposed by introducing the concepts of the 'look-ahead angle' and the 'radially shifted distance'. Tight path tracking can be made for any desired path defined as a space curve satisfying some suitable smoothness condition.

This paper is organized as follows. Path-following problem is formulated in Section 2, and a path-following guidance law is proposed in Section 3. The performance of the proposed guidance law is verified by numerical simulation in Section 4. Conclusion is given in Section 5.

2. PROBLEM FORMULATION

The following assumptions are required to design the path-following guidance law.

Assumption 1. (Smoothness Condition of Desired Path). The desired path is a parameterized, twice differentiable space curve.

Assumption 2. (Uniqueness of Reference Point). A closest projection point on a desired path can be uniquely determined as a reference point.

Assumption 3. (Direction of Unit Tangent Vector). The direction of the unit tangent vector of the desired path is determined by the desired path-following direction.

Figure 1 shows the geometry of the three-dimensional path-following problem and illustrates the Frenet-Serret frame of the desired path. In Fig. 1, P is a closest projection point on the desired path, M is a vehicle, $\mathbf{r}$ is a position vector defined in the inertial frame, $\mathbf{v}$ is a velocity vector, $(\hat{\mathbf{T}}, \hat{\mathbf{N}}, \hat{\mathbf{B}})$ are unit tangent, normal, and binormal vectors of the Frenet-Serret frame, $\mathbf{p}(l)$ is a desired path parameterized by l, and s and σ are distance along the desired path and the vehicle path, respectively.

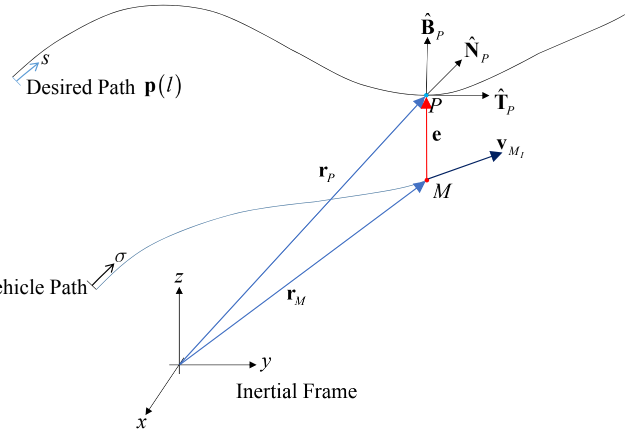

Fig. 1. Geometry of 3-D Path-Following

Definition 1. (Closest Projection Point P). For a given desired path $\mathbf{p}(l)$, the closest projection point(footpoint) P is defined as follows

$$\mathbf{r}_P\left(s\left(\sigma\right)\right) = \arg\min_{\mathbf{r}\in\mathbf{p}} \left\|\mathbf{r}_M\left(\sigma\right) - \mathbf{r}\right\| \tag{1}$$

where $\mathbf{e} \triangleq \mathbf{r}_P - \mathbf{r}_M$.

For the closest projection point defined by Eq. (1), the following condition is satisfied.

$$\mathbf{e} \perp \hat{\mathbf{T}}_P \tag{2}$$

It is assumed that the vehicle has an inner-loop controller that produces an exact acceleration as commanded by the guidance law, that is $\mathbf{a}_M = \mathbf{a}_{M_{\mathrm{cmd}}}$. The path-following problem can be mathematically defined as follows.

Definition 2. (Path-Following Problem). Design a guidance command $\mathbf{a}_{M_{\mathrm{cmd}}}$ such that the following conditions are satisfied for a vehicle as $\sigma \to \infty$.

$$\left\|\mathbf{r}_M\left(\sigma\right) - \mathbf{r}_P\left(s\left(\sigma\right)\right)\right\| \to 0 \tag{3}$$

$$\hat{\mathbf{T}}_M\left(\sigma\right) \to \hat{\mathbf{T}}_P\left(s\left(\sigma\right)\right) \tag{4}$$

If (3) is satisfied, the path of the vehicle will merge into the desired path, i.e., a position convergence. If (4) is satisfied, the vehicle will follow the direction of the desired path, i.e., a velocity direction convergence.

Also, "On-Track" and "Aligned" are defined as follows.

Definition 3. The vehicle is *On-Track*, if $\mathbf{r}_M = \mathbf{r}_P$.

Definition 4. The vehicle is *Aligned*, if $\hat{\mathbf{T}}_M = \hat{\mathbf{T}}_P$.

2.1 Differential Geometry of Space Curves

In this study, a modified Frenet-Serret frame is used for description of the motion along the desired path curve.

The velocity and the acceleration of a particle along a space curve can be represented as follows

$$\mathbf{v} = \left\|\mathbf{v}\right\| \hat{\mathbf{T}} = v\hat{\mathbf{T}} \tag{5}$$

$$\mathbf{a} = \dot{\mathbf{v}} = \dot{v}\hat{\mathbf{T}} + \kappa v^2 \hat{\mathbf{N}} \tag{6}$$

where κ is the curvature.

Remark 1. (Speed and Shape of a Space Curve). The shape of a space curve depends only on the curvature. The speed along the curve does not affect the shape of the curve. Therefore, the normal acceleration component $\kappa v^2 \hat{\mathbf{N}}$ in Eq. (6) determines the shape of the curve.

Remark 2. (Binormal Component of Acceleration). Due to Eq. (6), acceleration along a space curve has no binormal component.

2.2 Exact Path-Following Condition

According to the Remarks 1 and 2, the acceleration command of the vehicle generated by the path-following guidance law should satisfy the following condition.

Definition 5. (Exact Path-Following Condition). To maintain the vehicle *On-Track* and *Aligned* for the exact path-following, following two command conditions should be satisfied.

$$\mathbf{a}^N_{M_{\mathrm{cmd}}} \cdot \hat{\mathbf{N}}_P \bigg|_{\substack{\mathbf{r}_M = \mathbf{r}_P \\ \hat{\mathbf{T}}_M = \hat{\mathbf{T}}_P}} = \kappa_P \left\|\mathbf{v}_{M_I}\right\|^2 \tag{7}$$

$$\mathbf{a}^N_{M_{\mathrm{cmd}}} \cdot \hat{\mathbf{B}}_P \bigg|_{\substack{\mathbf{r}_M = \mathbf{r}_P \\ \hat{\mathbf{T}}_M = \hat{\mathbf{T}}_P}} = 0 \tag{8}$$

where $\mathbf{a}^N_{M_{\mathrm{cmd}}}$ is the command for normal acceleration which will be explained below.

Equation (7) implies that the curvature of the vehicle path should be equal to the curvature of the desired path, and Eq. (8) means that the acceleration of the vehicle should not have any component binormal to the desired path.

3. GUIDANCE LAW

3.1 Form of the Guidance Law

Let us consider Fig. 2 which shows the geometry of the guidance law considered in this study. The nonlinear path-following guidance law is proposed as follows.

$$\mathbf{a}^N_{M_{\mathrm{cmd}}} = k\left(\mathbf{v}_{M_I} \times \hat{\mathbf{L}}\right) \times \mathbf{v}_{M_I} \tag{9}$$

where $\mathbf{a}^N_{M_{\mathrm{cmd}}}$ is a 'normal guidance command', $k > 0$ is a guidance gain, $\mathbf{v}_{M_I}$ is an inertial velocity of the vehicle, and $\hat{\mathbf{L}}$ is a look-ahead vector. The 'normal guidance command' is a guidance command for 'normal acceleration' which is the component of acceleration perpendicular to the inertial velocity. As shown in Fig. 2, a geometric interpretation of the look-ahead vector $\hat{\mathbf{L}}$ is a unit vector which is rotated from the direction of $\mathbf{d}$ to the direction of $\hat{\mathbf{T}}_P$ by an angle θ_L.

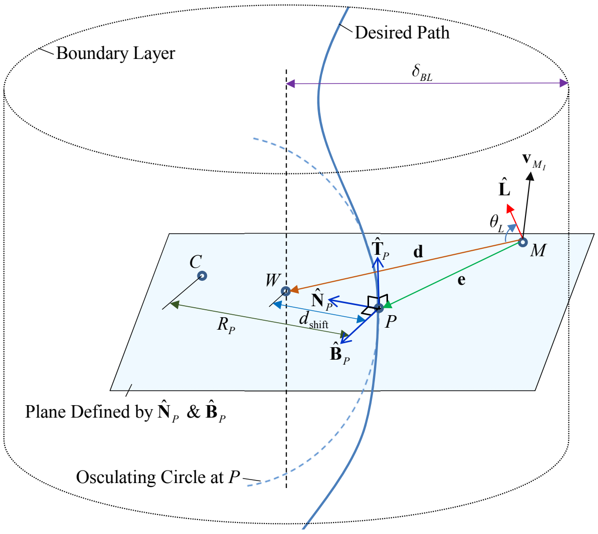

Fig. 2. Guidance Geometry

Theorem 1. (Guidance Law).
The normal acceleration $\mathbf{a}_M^N \triangleq \mathbf{a}_M - \left(\mathbf{a}_M \cdot \frac{\mathbf{v}_{M_I}}{v_{M_I}}\right)\frac{\mathbf{v}_{M_I}}{v_{M_I}}$ can be expressed by the following vector triple product

$$\begin{aligned}\mathbf{a}_M^N &= \kappa_M {v_{M_I}}^2 \hat{\mathbf{N}}_M \\ &= \left(\mathbf{v}_{M_I} \times \left(\kappa_M \hat{\mathbf{N}}_M + T\hat{\mathbf{T}}_M\right)\right) \times \mathbf{v}_{M_I}\end{aligned} \tag{10}$$

where $T \in \mathbb{R}$ is arbitrary.

Proof. Note from Eq. (5) that $\mathbf{v}_{M_I} = v_{M_I}\hat{\mathbf{T}}_M$, and $\mathbf{a}_M = \dot{v}_{M_I}\hat{\mathbf{T}}_M + \kappa_M {v_{M_I}}^2\hat{\mathbf{N}}_M$ from Eq. (6), therefore we have

$$\mathbf{a}_M^N = \mathbf{a}_M - \left(\mathbf{a}_M \cdot \hat{\mathbf{T}}_M\right)\hat{\mathbf{T}}_M = \kappa_M {v_{M_I}}^2 \hat{\mathbf{N}}_M \tag{11}$$

Rewriting Eq. (11) gives

$$\mathbf{a}_M^N = \kappa_M \left(\mathbf{v}_{M_I} \cdot \mathbf{v}_{M_I}\right)\hat{\mathbf{N}}_M \tag{12}$$

Using the fact $\mathbf{v}_{M_I} \cdot \hat{\mathbf{N}}_M = 0$ and $\left(\mathbf{v}_{M_I} \cdot T\hat{\mathbf{T}}_M\right)\mathbf{v}_{M_I} = \left(\mathbf{v}_{M_I} \cdot \mathbf{v}_{M_I}\right)T\hat{\mathbf{T}}_M$ for some $T \in \mathbb{R}$, Eq. (12) can be rewritten as follows.

$$\begin{aligned}\mathbf{a}_M^N =& -\left(\mathbf{v}_{M_I} \cdot \kappa_M \hat{\mathbf{N}}_M\right)\mathbf{v}_{M_I} + \left(\mathbf{v}_{M_I} \cdot \mathbf{v}_{M_I}\right)\kappa_M \hat{\mathbf{N}}_M \\ &- \left(\mathbf{v}_{M_I} \cdot T\hat{\mathbf{T}}_M\right)\mathbf{v}_{M_I} + \left(\mathbf{v}_{M_I} \cdot \mathbf{v}_{M_I}\right)T\hat{\mathbf{T}}_M \\ =& -\left(\mathbf{v}_{M_I} \cdot \left(\kappa_M \hat{\mathbf{N}}_M + T\hat{\mathbf{T}}_M\right)\right)\mathbf{v}_{M_I} \\ &+ \left(\mathbf{v}_{M_I} \cdot \mathbf{v}_{M_I}\right)\left(\kappa_M \hat{\mathbf{N}}_M + T\hat{\mathbf{T}}_M\right) \\ =& \left(\mathbf{v}_{M_I} \times \left(\kappa_M \hat{\mathbf{N}}_M + T\hat{\mathbf{T}}_M\right)\right) \times \mathbf{v}_{M_I}\end{aligned} \tag{13}$$

□

Using Theorem 1, the normal acceleration command can be generated by the triple product of $\mathbf{v}_{M_I}$ and a vector $\mathbf{q}$ corresponding to $\kappa_M \hat{\mathbf{N}}_M + T\hat{\mathbf{T}}_M$. Therefore, a guidance law can be constructed by the proper selection of $\mathbf{q}$. In this study, $k\hat{\mathbf{L}}$ is proposed for $\mathbf{q}$ to realize the look-ahead effect, which is explained in detail below.

Corollary 1. (Direction of the Guidance Command).
If $\mathbf{a}_M^N = \mathbf{a}_{M_{\text{cmd}}}^N$, then the direction of the guidance command can be represented as

$$\frac{\mathbf{a}_{M_{\text{cmd}}}^N}{\left\|\mathbf{a}_{M_{\text{cmd}}}^N\right\|} = \text{sign}\left(\kappa_M\right)\hat{\mathbf{N}}_M = \frac{k}{|\kappa_M|}\text{rej}(\hat{\mathbf{L}}, \mathbf{v}_{M_I}) \tag{14}$$

where $\text{rej}(\mathbf{a}, \mathbf{b}) = \mathbf{a} - \frac{\mathbf{a}\cdot\mathbf{b}}{\|\mathbf{b}\|}\frac{\mathbf{b}}{\|\mathbf{b}\|}$, which is the vector component of $\mathbf{a}$ perpendicular to $\mathbf{b}$, as shown in Fig. 3.

Proof. By Eqs. (9) and (10), the direction vector of $\mathbf{a}_{M_{\text{cmd}}}^N$ can be written as

$$\begin{aligned}\frac{\mathbf{a}_{M_{\text{cmd}}}^N}{\left\|\mathbf{a}_{M_{\text{cmd}}}^N\right\|} &= \frac{k\left(\mathbf{v}_{M_I} \times \hat{\mathbf{L}}\right) \times \mathbf{v}_{M_I}}{\left\|\kappa_M {v_{M_I}}^2\hat{\mathbf{N}}_M\right\|} \\ &= \frac{k\left(-\left(\mathbf{v}_{M_I} \cdot \hat{\mathbf{L}}\right)\mathbf{v}_{M_I} + \left(\mathbf{v}_{M_I} \cdot \mathbf{v}_{M_I}\right)\hat{\mathbf{L}}\right)}{\left\|\kappa_M {v_{M_I}}^2\hat{\mathbf{N}}_M\right\|} \\ &= \frac{k}{|\kappa_M|}\left(\hat{\mathbf{L}} - \frac{\left(\hat{\mathbf{L}} \cdot \mathbf{v}_{M_I}\right)}{v_{M_I}}\frac{\mathbf{v}_{M_I}}{v_{M_I}}\right) \\ &= \frac{k}{|\kappa_M|}\text{rej}(\hat{\mathbf{L}}, \mathbf{v}_{M_I})\end{aligned} \tag{15}$$

□

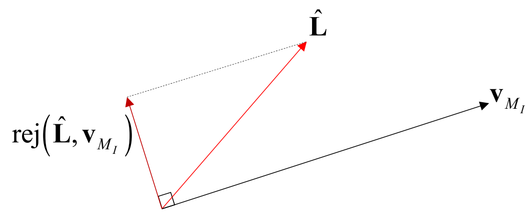

Fig. 3. Direction of the Guidance Command

Remark 3. (Look-Ahead Effect).
It can be stated from Corollary 1 that the vehicle with the proposed guidance law, Eq. (9), tends to align its inertial velocity $\mathbf{v}_{M_I}$ with the look-ahead vector $\hat{\mathbf{L}}$. This feature, named 'look-ahead effect', originates from the property of the pursuit guidance.

3.2 Construction of the Look-Ahead Vector

The look-ahead vector $\hat{\mathbf{L}}$ is constructed by θ_L and d_{shift} as shown in Fig. 2. In the Fig. 2, C is the center of curvature at P, W is a point defined on the line from P to C. Therefore, $\mathbf{r}_W$ can be represented as

$$\mathbf{r}_W \triangleq \mathbf{r}_P + d_{\text{shift}}\text{sign}\left(\kappa_P\right)\hat{\mathbf{N}}_P \tag{16}$$

where d_{shift} is a 'radially shifted distance'. Since $\mathbf{e} = \mathbf{r}_P - \mathbf{r}_M$, the distance vector from M to W can be represented as

$$\mathbf{d} \triangleq \mathbf{r}_W - \mathbf{r}_M = \mathbf{e} + d_{\text{shift}}\text{sign}\left(\kappa_P\right)\hat{\mathbf{N}}_P \tag{17}$$

Let $\hat{\mathbf{d}} \triangleq \frac{\mathbf{d}}{\|\mathbf{d}\|}$, then the look-ahead vector $\hat{\mathbf{L}}$ can be constructed as follows

$$\hat{\mathbf{L}} \triangleq \cos\theta_L\hat{\mathbf{d}} + \sin\theta_L\hat{\mathbf{T}}_P \tag{18}$$

where θ_L is the 'look-ahead angle' which will be defined in the following subsection.

3.2.1 Radially Shifted Distance (d_{shift})
An additional degree-of-freedom in the proposed guidance law comes from the introduction of radially shifted distance, which is included to generate accurate acceleration command for exact path-following. The value of d_{shift} is determined by the value that satisfies the *Exact Path-Following Condition* as stated in Def. 5.

If the vehicle is *On-Track*, then $\mathbf{e} = \mathbf{0}$, and $\mathbf{d}|_{\mathbf{e}=\mathbf{0}} = d_{\text{shift}} \text{sign}(\kappa_P) \hat{\mathbf{N}}_P$. Therefore, we have

$$\begin{aligned} \hat{\mathbf{L}}\Big|_{\mathbf{e}=\mathbf{0}} &= \cos\left(\theta_L\left(\|\mathbf{d}|_{\mathbf{e}=\mathbf{0}}\|\right)\right)\hat{\mathbf{d}}\Big|_{\mathbf{e}=\mathbf{0}} + \sin\left(\theta_L\left(\|\mathbf{d}|_{\mathbf{e}=\mathbf{0}}\|\right)\right)\hat{\mathbf{T}}_P \\ &= \cos\left(\theta_L\left(d_{\text{shift}}\right)\right)\text{sign}\left(\kappa_P\right)\hat{\mathbf{N}}_P + \sin\left(\theta_L\left(d_{\text{shift}}\right)\right)\hat{\mathbf{T}}_P \end{aligned} \tag{19}$$

where θ_L is designed as a function of $\|\mathbf{d}\|$.

In addition to *On-Track*, if the vehicle is also *Aligned*, $\hat{\mathbf{T}}_M = \hat{\mathbf{T}}_P$, then we have

$$\mathbf{v}_{M_I}|_{\hat{\mathbf{T}}_M=\hat{\mathbf{T}}_P} = \|\mathbf{v}_{M_I}\|\,\hat{\mathbf{T}}_P \tag{20}$$

Substituting Eqs. (19) and (20) into the proposed guidance law of Eq. (9), the command generated at the *On-Track* and *Aligned* condition can be represented as follows.

$$\begin{aligned} \mathbf{a}^N_{M_{\text{cmd}}}\Big|_{\substack{\mathbf{e}=\mathbf{0} \\ \hat{\mathbf{T}}_M=\hat{\mathbf{T}}_P}} &= k\left(\mathbf{v}_{M_I}|_{\hat{\mathbf{T}}_M=\hat{\mathbf{T}}_P} \times \hat{\mathbf{L}}\Big|_{\mathbf{e}=\mathbf{0}}\right) \times \mathbf{v}_{M_I}|_{\hat{\mathbf{T}}_M=\hat{\mathbf{T}}_P} \\ &= k\,\|\mathbf{v}_{M_I}\|^2 \cos\left(\theta_L\left(d_{\text{shift}}\right)\right)\text{sign}\left(\kappa_P\right)\hat{\mathbf{N}}_P \end{aligned} \tag{21}$$

Note that Eq. (8) is satisfied by Eq. (21). Also, the guidance command Eq. (21) should satisfy Eq. (7) as follows.

$$\begin{aligned} \mathbf{a}^N_{M_{\text{cmd}}} \cdot \hat{\mathbf{N}}_P\Big|_{\substack{\mathbf{e}=\mathbf{0} \\ \hat{\mathbf{T}}_M=\hat{\mathbf{T}}_P}} &= k\,\|\mathbf{v}_{M_I}\|^2 \cos\left(\theta_L\left(d_{\text{shift}}\right)\right)\text{sign}\left(\kappa_P\right) \\ &= \kappa_P\,\|\mathbf{v}_{M_I}\|^2 \end{aligned} \tag{22}$$

Therefore, d_{shift} should satisfy the following condition for exact path-following.

$$d_{\text{shift}} = \left\{ x \geq 0 : \theta_L(x) = \cos^{-1}\left(\frac{|\kappa_P|}{k}\right) \right\} \tag{23}$$

3.2.2 Look-Ahead Angle (θ_L)
The look-ahead angle θ_L should satisfy several conditions to realize the look-ahead effect for the path-following. Consider a virtual tube of constant radius δ_{BL} around the axis which penetrates W and is parallel to $\hat{\mathbf{T}}_P$ as shown in Fig. 2. Let us call this tube as a 'boundary layer' so that δ_{BL} is the 'boundary layer thickness'. Considering Remark 3 in mind, it can be summarized that

(1) θ_L should be a function of $\|\mathbf{d}\|$
(2) $\frac{d\theta_L(\|\mathbf{d}\|)}{d\|\mathbf{d}\|} < 0$ inside the boundary layer $(\|\mathbf{d}\| < \delta_{BL})$ to steer the velocity to the direction tangential to the desired path,
(3) $\frac{d^2\theta_L(\|\mathbf{d}\|)}{d\|\mathbf{d}\|^2} < 0$ inside the boundary layer for smooth incidence to the desired path,
(4) $\theta_L(\|\mathbf{d}\|) = 0$ outside the boundary layer $(\|\mathbf{d}\| > \delta_{BL})$ to make the vehicle approach to the desired path as fast as possible,
(5) $\theta_L(\|\mathbf{d}\| = 0) = \frac{\pi}{2}$[rad] and $\theta_L(\|\mathbf{d}\| = \delta_{BL}) = 0$[rad] to satisfy the boundary conditions.

Various functions satisfying the above conditions may be introduced. In this study, following two look-ahead angle functions are proposed.

$$\theta_L\left(\|\mathbf{d}\|\right) = \frac{\pi}{2}\sqrt{1 - \frac{\|\mathbf{d}\|}{\delta_{BL}}} \tag{24}$$

$$\theta_L\left(\|\mathbf{d}\|\right) = \cos^{-1}\left(\frac{\|\mathbf{d}\|}{\delta_{BL}}\right) \tag{25}$$

Figure 4 shows the shapes of the above two look-ahead angle functions.

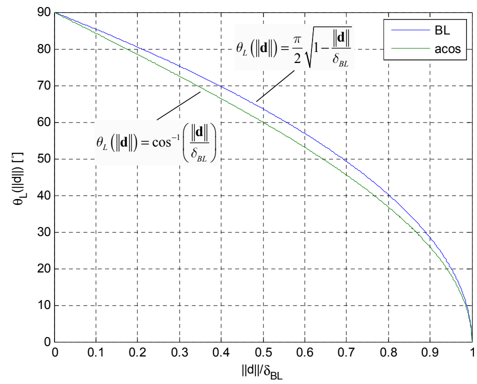

Fig. 4. Look-Ahead Angle Function

Note that if the look-ahead angle function given by Eq. (24) is used, d_{shift} can be expressed as

$$d_{\text{shift}} = \left[1 - \left(\frac{2}{\pi}\cos^{-1}\left(\frac{|\kappa_P|}{k}\right)\right)^2\right]\delta_{BL} \tag{26}$$

On the other hand, if Eq. (25) is used, d_{shift} can be expressed as

$$d_{\text{shift}} = \frac{|\kappa_P|}{k}\delta_{BL} \tag{27}$$

3.3 Properties of the Proposed Guidance Law

Note that the magnitude of the guidance command is bounded by $\mathbf{a}^N_{M_{\text{cmd}}} \leq k\,\|\mathbf{v}_{M_I}\|^2$. There are only two design parameters, k and δ_{BL}, in the proposed guidance law. The guidance gain k affects the amount of the command. If the initial position of the vehicle is outside of the boundary layer, the boundary layer thickness δ_{BL} determines where the vehicle begins to steer its velocity to the direction of the desired path. The proposed guidance law is all-aspect, and therefore autonomous flight mode can be engaged regardless of the initial vehicle position. Also, the proposed guidance law is nonsingular except the case that Assumption 2 does not hold, i.e. at the center of a circle.

The core difference between the proposed guidance law and existing look-ahead point based guidance law is that the proposed guidance law realized the look-ahead effect by the look-ahead angle, not by the look-ahead point.

Look-Ahead Point based Method :
A look-ahead point based path-following guidance law proposed in Park et al. (2007) is given as follows

$$\mathbf{a}^N_{M_{\text{cmd}}} = \frac{2}{\|\mathbf{L}\|^2}\left(\mathbf{v}_{M_I} \times \mathbf{L}\right) \times \mathbf{v}_{M_I} \tag{28}$$

where $\mathbf{L}$ is the look-ahead vector defined by the relative position vector of the look-ahead point on the desired path, which is ahead of the vehicle by the specified distance L with respect to the vehicle. This guidance law cannot satisfy the *Exact Path-Following Condition* when the desired path is not a two-dimensional curve of constant curvature. It is because that, even if the vehicle is *On-Track* and *Aligned*, the followings are observed.

1) $\kappa_M = \frac{1}{\|\mathbf{L}\|} \neq \kappa_P$, therefore $\mathbf{a}_{M_{\text{cmd}}} \cdot \hat{\mathbf{N}}_P \neq \kappa_P \|\mathbf{v}_{M_I}\|^2$,

2) $\mathbf{L} \cdot \hat{\mathbf{B}}_P \neq 0$, therefore $\mathbf{a}_{M_{\text{cmd}}} \cdot \hat{\mathbf{B}}_P \neq 0$.

3.4 Modification for Constant Airspeed Path-Following

When the wind velocity $\mathbf{v}_w$ is not zero, the inertial velocity $\mathbf{v}_{M_I}$ is not equal to the relative velocity $\mathbf{v}_{M_a} = \mathbf{v}_{M_I} - \mathbf{v}_w$, due to the wind. Therefore, the normal guidance command $\mathbf{a}^N_{M_{\text{cmd}}}$ has a component tangential to $\mathbf{v}_{M_a}$, which is not desirable because it is not easy to change the airspeed in practice. Note that maintaining constant airspeed is better than maintaining constant ground speed.

Let $\mathbf{a}^S_{M_{\text{cmd}}}$ is the 'side guidance command' which is modified from the normal guidance command $\mathbf{a}^N_{M_{\text{cmd}}}$ by the following command modifying logic.

To maintain constant airspeed, the acceleration of the vehicle should be orthogonal to the relative velocity $\mathbf{v}_{M_a}$, so that the following condition should be satisfied.

$$\mathbf{a}^S_{M_{\text{cmd}}} \cdot \mathbf{v}_{M_a} = 0 \tag{29}$$

As explained in Remark 1, the shape of the curve only depends on the normal acceleration, not on the inertial speed along the curve. Thus, whatever the tangential acceleration is, the normal acceleration should be equal to Eq. (9) to preserve the path-following ability. Therefore, the following condition should be satisfied.

$$\left(\mathbf{a}^S_{M_{\text{cmd}}} \cdot \frac{\mathbf{a}^N_{M_{\text{cmd}}}}{\|\mathbf{a}^N_{M_{\text{cmd}}}\|}\right) \frac{\mathbf{a}^N_{M_{\text{cmd}}}}{\|\mathbf{a}^N_{M_{\text{cmd}}}\|} = \mathbf{a}^N_{M_{\text{cmd}}} \tag{30}$$

Rewriting Eq. (30) gives

$$\mathbf{a}^S_{M_{\text{cmd}}} \cdot \mathbf{a}^N_{M_{\text{cmd}}} = \|\mathbf{a}^N_{M_{\text{cmd}}}\|^2 \tag{31}$$

The side guidance command should lie in the plane defined by $\mathbf{v}_{M_I}$ and $\mathbf{a}^N_{M_{\text{cmd}}}$ to avoid the generation of binormal component, therefore

$$\mathbf{a}^S_{M_{\text{cmd}}} \cdot \left(\mathbf{v}_{M_I} \times \mathbf{a}^N_{M_{\text{cmd}}}\right) = 0 \tag{32}$$

Let us rewrite Eqs. (29), (31), and (32) into a matrix equation as follows

$$\begin{bmatrix} \mathbf{v}_{M_a}{}^T \\ \mathbf{a}^N_{M_{\text{cmd}}}{}^T \\ \left(\mathbf{v}_{M_I} \times \mathbf{a}^N_{M_{\text{cmd}}}\right)^T \end{bmatrix} \mathbf{a}^S_{M_{\text{cmd}}} = \begin{bmatrix} 0 \\ \|\mathbf{a}^N_{M_{\text{cmd}}}\|^2 \\ 0 \end{bmatrix} \tag{33}$$

Finally, the modified side guidance command can be given as follows

$$\mathbf{a}^S_{M_{\text{cmd}}} = \begin{cases} \begin{bmatrix} \mathbf{v}_{M_a}{}^T \\ \mathbf{a}^N_{M_{\text{cmd}}}{}^T \\ \left(\mathbf{v}_{M_I} \times \mathbf{a}^N_{M_{\text{cmd}}}\right)^T \end{bmatrix}^{-1} \begin{bmatrix} 0 \\ \|\mathbf{a}^N_{M_{\text{cmd}}}\|^2 \\ 0 \end{bmatrix} \\ \quad \text{if } \mathbf{v}_{M_I} \cdot \mathbf{v}_{M_a} \neq \mathbf{0} \text{ and } \mathbf{a}^N_{M_{\text{cmd}}} \neq \mathbf{0} \\ \mathbf{0} \quad \text{if } \mathbf{v}_{M_I} \cdot \mathbf{v}_{M_a} = \mathbf{0} \text{ or } \mathbf{a}^N_{M_{\text{cmd}}} = \mathbf{0} \end{cases} \tag{34}$$

Corollary 2. (Nonsingularity of the Matrix).

If $\mathbf{v}_{M_I} \cdot \mathbf{v}_{M_a} \neq \mathbf{0}$ and $\mathbf{a}^N_{M_{\text{cmd}}} \neq \mathbf{0}$, then $\begin{bmatrix} \mathbf{v}_{M_a}{}^T \\ \mathbf{a}^N_{M_{\text{cmd}}}{}^T \\ \left(\mathbf{v}_{M_I} \times \mathbf{a}^N_{M_{\text{cmd}}}\right)^T \end{bmatrix}$ in Eq. (34) is always nonsingular.

Proof. Let $\mathbf{v}_{M_I} = \left[v_{I_x}\ v_{I_y}\ v_{I_z}\right]^T$, $\mathbf{v}_{M_a} = \left[v_{a_x}\ v_{a_y}\ v_{a_z}\right]^T$, and $\mathbf{a}^N_{M_{\text{cmd}}} = \left[a_x\ a_y\ a_z\right]^T$, which satisfy

$$\mathbf{a}^N_{M_{\text{cmd}}} \cdot \mathbf{v}_{M_I} = a_x v_{I_x} + a_y v_{I_y} + a_z v_{I_z} = 0 \tag{35}$$

Using Eq. (35), we have

$$\begin{vmatrix} \mathbf{v}_{M_a}{}^T \\ \mathbf{a}^N_{M_{\text{cmd}}}{}^T \\ \left(\mathbf{v}_{M_I} \times \mathbf{a}^N_{M_{\text{cmd}}}\right)^T \end{vmatrix} = \|\mathbf{a}^N_{M_{\text{cmd}}}\|^2 \left(\mathbf{v}_{M_I} \cdot \mathbf{v}_{M_a}\right) \tag{36}$$

Equation (36) shows that the determinant is not zero if and only if $\mathbf{v}_{M_I} \cdot \mathbf{v}_{M_a} \neq \mathbf{0}$ and $\mathbf{a}^N_{M_{\text{cmd}}} \neq \mathbf{0}$.

□

Figure 5 shows the flowchart of the proposed guidance law.

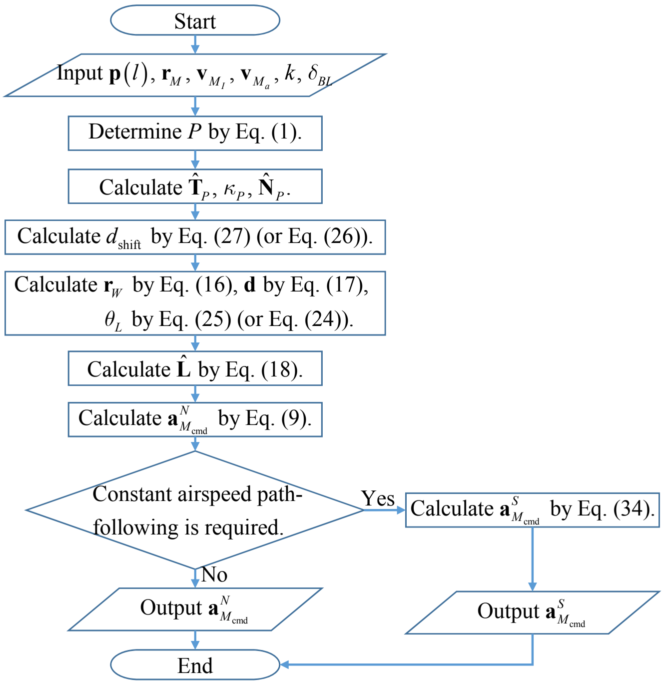

Fig. 5. Flowchart of the Guidance Law

4. NUMERICAL SIMULATION

Numerical simulation is performed to verify the performance of the proposed guidance law. Numerical simulation using the existing method (Park et al. (2007); Eq. (28)) [1] is also performed to compare the path-tracking performance.

3-DOF fixed-wing aircraft coordinated flight model is used, and the simulation parameters are summarized in Table 1.

[1] L in Table 1 is the look-ahead distance which is the design parameter of Park's method.

Table 1. Simulation Parameters [mks units]

$\mathbf{r}_M(t_0) = \begin{bmatrix} 140 \\ 0 \\ 20\pi + 2 \end{bmatrix}$	$\mathbf{v}_{M_I}(t_0) = \begin{bmatrix} 4.3412 \\ 24.6202 \\ 0 \end{bmatrix}$	$\mathbf{v}_w = \begin{bmatrix} 5 \\ 0 \\ 0 \end{bmatrix}$
$k = 0.015$	$\delta_{BL} = 100$	$L = 150$

Desired path for the simulation is a helix defined as follows

$$\mathbf{p}(l) = \begin{bmatrix} 100\cos l \\ 100\sin l \\ 10l \end{bmatrix} \tag{37}$$

Figures 6 and 7 show the trajectories and guidance command histories using the proposed guidance law and the existing method, respectively. The time histories of the cross-track error $\|\mathbf{e}\|$ are shown in Fig. 8. It can be concluded from Fig. 8 that the cross-track error converges to zero with the proposed guidance law, but not with the existing method. The amount of the guidance command is similar in both methods as shown in Fig. 7. The performance index value of the proposed method is $J = 328.18$, and that of the existing method is $J = 1,016.45$. Thus, it can be concluded that the tracking performance of the proposed guidance law is better than that of the existing method.

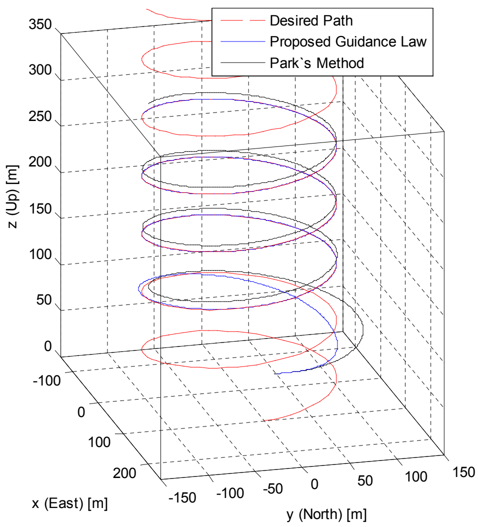

Fig. 6. 3-D Trajectory

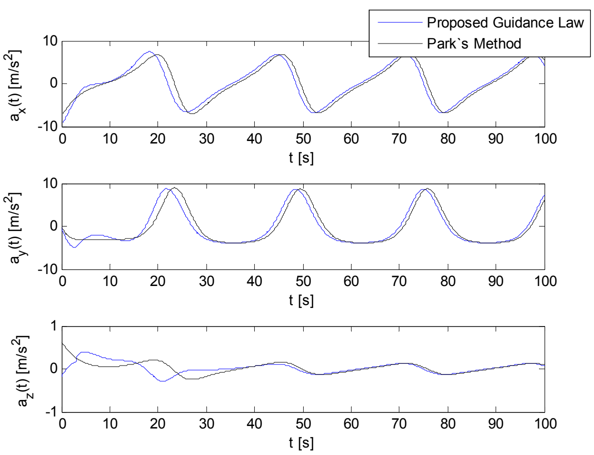

Fig. 7. Guidance Command History

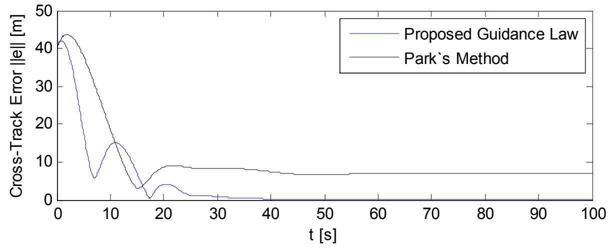

Fig. 8. Cross-Track Error History

5. CONCLUSION

A three-dimensional nonlinear path-following guidance law was proposed. The proposed guidance law maintained the major advantages of existing methods, but overcame the weaknesses. Precise path-following for a general desired path can be achieved. For future works, the stability and performance analysis will be performed. The guideline for the selection of the design parameter will be given. And the effectiveness of the guidance law will be demonstrated by flight experiments.

ACKNOWLEDGEMENTS

This work was supported by a Defense Research Grant, funded by the Agency for Defense Development, under the contract UD120013JD.

REFERENCES

Cabecinhas, D., Silvestre, C., Rosa, P., and Cunha, R. (2007). Path-Following Control for Coordinated Turn Aircraft Maneuvers. *AIAA Guidance, Navigation, and Control Conference*. Hilton Head, SC.

Curry, R., Lizarraga, M., Mairs, B., and Elkaim, G.H. (2013). L_2^+, an Improved Line of Sight Guidance Law for UAVs. *American Control Conference*. Washington, DC.

Gates, D.J. (2010). Nonlinear Path Following Method. *Journal of Guidance, Control, and Dynamics*, 33(2), 321–332.

Lawrence, D.A., Frew, E.W., and Pisano, W.J. (2008). Lyapunov Vector Fields for Autonomous Unmanned Aircraft Flight Control. *Journal of Guidance, Control, and Dynamics*, 31(5), 1220–1229.

Nelson, D.R., Barber, D.B., McLain, T.W., and Beard, R.W. (2007). Vector Field Path-Following for Miniature Air Vehicles. *IEEE Transactions on Robotics and Automation*, 23(3), 519–529.

Park, S., Deyst, J., and How, J.P. (2007). Performance and Lyapunov Stability of a Nonlinear Path-Following Guidance Method. *Journal of Guidance, Control, and Dynamics*, 30(6), 1718–1728.

Yamasaki, T., Balakrishnan, S.N., and Takano, H. (2013). Separate-Channel Integrated Guidance and Autopilot for Automatic Path-Following. *Journal of Guidance, Control, and Dynamics*, 36(1), 25–34.